International Journal of Biological Macromolecules 257 (2024) 128705

Contents lists available at ScienceDirect

International Journal of Biological Macromolecules

journal homepage: www.elsevier.com/locate/ijbiomac

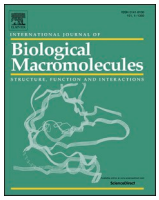

G-POSS connected double network starch gels for protein release

Seyma Nur Kirmic Cosgun, Deniz Ceylan Tuncaboylu *, Mahinur Alemdar

Bezmialem Vakıf University Health Sciences Institute, Department of Biotechnology, 34093 Istanbul, Turkey
Bezmialem Vakif University, Faculty of Pharmacy, 34093 Istanbul, Turkey

ARTICLE INFO

Keywords:
Glycidyl-POSS
Starch
Hydrogel
Nanocomposite
Protein release
Double network

ABSTRACT

Starch is one of the most frequently preferred natural polymers in hydrogel synthesis. Herein, we combined two strategies of associating brittle and ductile networks in a structure and incorporating inorganic particles into the polymeric gel to design mechanically enhanced nanocomposite double network (DN) starch gels. For the first time in the literature, nanocomposite starch gels (s-NC) were designed by cross-linking starch chains with 8-armed glycidyl-polyhedral oligomeric silsesquioxane (g-POSS) units. Fourier Transform Infrared Spectroscopy and Energy Dispersive X-Ray Spectroscopy analyses have proven that g-POSS is included in the gel structure and is homogeneously distributed throughout the network. More stable d-NC-DMA and d-NC-VP gels were obtained by incorporating *N,N*-dimethylacrylamide (DMA), or 1-vinyl-2-pyrrolidinone (VP) units, respectively, into g-POSS-linked starch gels, and the reaction kinetics were followed *in situ*. In SEM images, it was observed that d-NC-DMA had smaller pores and thicker pore walls compared to s-NC and d-NC-VP starch gels, and its mechanical strength was shown to be much superior by rheological tests, compression, and tensile analyses. In addition to increasing the mechanical strength of the gels, the potential of starch in protein release applications using amylase sensitivity has been demonstrated *in vitro* experiments using the model protein BSA.

1. Introduction

Hydrogels are chemically and/or physically cross-linked 3-dimensional polymeric networks that swell in water. The fact that hydrogels, mostly composed of water (>90 %), maybe both be bio-compatible and can be used in many ways, have increased their applications [1–3]. It is possible to obtain hydrogels with different cross-linking methods using natural and synthetic polymers and monomers. Polysaccharides such as starch, dextran, hyaluronic acid and chitosan are the most preferred natural polymers in hydrogel synthesis with their bio-compatible and degradable characteristics [4,5]. Starch is a non-toxic polysaccharide mainly composed of amylose (Amy) and amylopectin (Amp) units as well as a small quantity of phospholipids and free fatty acids in the structure. Amy with a molecular weight of about $\times 10^6$ is a linear homopolymer, while the molecular weight of branched Amp is around $\times 10^8$ [6]. High molecular weight and branched structure reduce the mobility of Amp chains and leads to less hydrogen bond formation in addition, it is well known that Amy has a better incorporation to associate [7]. Amy/Amp ratios in the structure vary depending on the source, and this directly affects the properties of starch such as solubility, gelation temperature and viscosity [4].

Depending on the application areas, it is possible to modify hydroxyl groups of starch to improve the properties [6,8]. Starch-based hydrogels can be obtained mainly in two different ways, by graft copolymerization of vinyl monomers in the presence of a crosslinker and by direct crosslinking [9]. Various crosslinking agents are used for covalent bonding of starch using hydroxyl groups on the chains such as glutaraldehyde (GA), epichlorohydrin (ECH), sodium trimetaphosphate (STMP), sodium tripolyphosphate (STPP), and phosphoryl chloride ($POCl_3$) [10,11]. Among other crosslinkers, ECH is the most widely used one in polysaccharide chemistry [12]. The alkaline environment (pH > 9) is important in activating the hydroxyl groups of starch during the nucleophilic attack of the crosslinker and contributes to the chain esterification reaction, which is responsible for the crosslinking of the material [13,14]. In addition, high temperature is required for starch to gelatinize in water, while pre-gelatinization is carried out at low temperature in an alkaline environment [15–19].

In many application areas of soft materials, it is essential that they have good mechanical properties. However, gels that swell in water are usually very brittle. To obtain a hydrogel with adjustable mechanical properties, it is necessary to incorporate molecular-level energy dissipation mechanisms throughout the gel sample, thereby increasing the

* Corresponding author.
E-mail address: dtuncaboylu@bezmialem.edu.tr (D. Ceylan Tuncaboylu).

https://doi.org/10.1016/j.ijbiomac.2023.128705
Received 9 September 2023; Received in revised form 27 November 2023; Accepted 7 December 2023
Available online 9 December 2023

viscoelastic distribution. Some of the methods commonly used in this direction are double network (DN) or triple network (TN) gels, topological gels, nanocomposite (NC) gels and cryogels [20–23]. Containing an organic polymer and an inorganic particle, NC gels have outstanding properties such as superior elongation, rapid swelling response to temperature changes, and high equilibrium swelling values. DN structures consist of two brittle and ductile (soft) networks interconnected in a single gel material. The sacrificial bonds of the brittle network break under low pressure to dissipate the energy and form many microcracks, while the ductile network holds the macroscopic sample together.

One of the structures used as a "nanostructure" unit to prepare new NC materials is poly(hedral oligomeric silsesquioxane) (POSS). Polyhedral and eight-armed POSS molecules with the general formula $(RSiO1.5)_n$ are non-toxic, have good biocompatibility and stability [24,25]. n ranges from 6 to 18, and the silica and oxygen atoms combine in a nucleus with inorganic silica-like geometry. The inorganic core of POSS is surrounded by organic ligands such as hydrogen, halogen, alkyl groups covalently bonded to Si atoms located at the corners of the polyhedral lattice [26]. An example of modified POSS structures is glycidyl-POSS (g-POSS) functionalized with epoxy groups [24]. In one study, it was suggested that functionalized cubic POSS with epoxy-terminated peak groups would facilitate the design of new materials with significant potential [27]. NC materials containing a small amount of POSS have been shown to have excellent material properties such as high thermal stability, good oxidation resistance, increased surface hardness and improved mechanical properties due to the high mechanical stability of nano-sized particles [28–30].

The frequency of use of pharmaceutical proteins, a class of therapeutic agents, has gradually increased after the introduction of insulin [31]. However, it is an important problem that such drug agents have short half-lives and are easily degraded by enzymes [32,33]. For this reason, biodegradable and biocompatible hydrogel-based carriers allow the loading of hydrophilic bioactive proteins at high concentrations with adjustable release profiles and ensure the preservation of the protein's structure [34]. In addition, physical and/or chemical degradation of the carrier is an important step to remove the carrier. Most of the physically degradable systems have been reported to occur *via* the enzymatic degradation mechanism of polymers. The most important point to note as a potential disadvantage of biodegradable polymers is the ultimate toxicity of the degradable products. For this reason, natural polymers that can be used as drug carriers and give non-toxic and biodegradable products are preferred for controlled release technology [35–39].

In this paper, two strategies of associating brittle and ductile networks in a structure and incorporating inorganic particles into the polymer network were combined to design mechanically enhanced nanocomposite double network starch gels. It has been shown by our research group that a significant improvement in the properties of starch gels is achieved by increasing the Amy/Amp ratio from 23 to 70 % [40]. For this reason, Hylon VII corn starch containing high amylose was used for experimental studies in order to obtain mechanically stronger gels. In the first step, nanocomposite starch gels were obtained by using g-POSS units as a crosslinker for the first time in the literature. In the second step, more stable DN starch gels were obtained by incorporating *N,N*-dimethylacrylamide (DMA) or 1-vinyl-2-pyrrolidinone (VP) units, which are hydrophilic monomers with good water uptake and low cytotoxicity, as a second networks into these NC gels [41]. The potential of the prepared gels in protein release applications was investigated by utilizing the enzyme sensitivity feature of starch.

2. Materials and methods

2.1. Materials

High amylose content corn starch (HYLON VII, ~70 % amylose content; 13 % moisture; 2.06×10^6 g/mol Molecular weight) was kindly provided by Ingredion Germany GmbH. Glycidyl-polyhedral oligomeric silsesquioxane (g-POSS) was purchased from Hybrid Plastics. Potassium hydroxide (KOH, Merck), *N, N*-dimethylacrylamide (DMA, Sigma-Aldrich), 1-vinyl-2-pyrrolidinone (VP, Sigma-Aldrich), *N,N′*-methylene (*bis*)acrylamide (BAAm, Sigma Aldrich), Tetrahydrofuran (THF, Merck) used as received. 2-Hydroxy-4′-(2-hydroxyethoxy)-2-methylpropiophenone (Irgacure 2959, Sigma Aldrich) was used as the photoinitiator. Bovine serum albumin (BSA) and *α*-amylase enzyme from Aspergillus oryzae were purchased from Sigma-Aldrich for use in protein release studies.

2.2. Hydrogel preparation

In a typical synthesis of single network nanocomposite starch gels (s-NC), starch granules (1 g) in a total volume of 8 mL were dissolved in KOH solution (0.0125 g/mL) at 70 °C and mixed for 15 min. In another vial, g-POSS (0.4 g) used as a crosslinker was dissolved in THF (2 mL) and then transferred into the starch-containing reaction vial. It was vortexed for a while to obtain a homogeneous solution. As a next step, the reaction solution was taken into glass molds containing a 1 mm thick Teflon spacer or cylindrical syringes. Reactions were performed in an oven at 50 °C for 24 h.

In order to enhance the mechanical properties of starch gels, d-NC gels with double network structure were prepared by using synthesized s-NC networks. The s-NC starch gel was immersed in a reaction solution containing DMA or VP monomers, BAAm crosslinker, and Irgacure photoinitiator. In the molds used in the first stage for gels, polymerization and cross-linking reactions after a certain period, were performed under UV light in a merry-go-round type photoreactor (Kerman Lab) equipped with 18 Philips 8 W lamps emitting light nominally at $\lambda = 365$ nm for 24 h. After reaction, double network gels containing DMA and VP were obtained, designated d-NC-DMA and d-NC-VP, respectively.

2.3. Characterization of hydrogels

2.3.1. Gel fraction

To determine gel fractions, s-NC starch gels were weighed after preparation. They were then placed in beakers containing distilled water, and their weight was monitored daily until to reached swelling equilibrium at 24 °C. The resulting insoluble gels were lyophilized to obtain constant dry weight. The gel fractions were obtained from the weight ratio between the insoluble dry gel weight and the initial weight of the gel. The same procedure was followed after the double-network gels were formed with the dry s-NC gels.

$$\text{Gel Fraction } (\%) = \left(m_{dry}/m_o\right) \times 100 \quad (1)$$

where m_{dry} and m_o are the weight of the insoluble dry gel and the weight of the gel after preparation [42].

2.3.2. FTIR

The FT-IR spectra of the lyophilized NC starch gels were measured in transmission mode with a Bruker Alpha FTIR infrared spectrometer in the range of 4000–400 cm^{-1}.

2.3.3. Scanning electron microscopy

Lyophilized dried gels were coated with Au/Pd before examining their morphology under high-resolution field emission scanning electron microscopy (JEOL SEM-7100-EDX) at 1 kV acceleration voltage. Elemental analyzes were performed with SEM-energy dispersed X-Ray spectroscopy Analysis (EDX). Images were acquired at 10, 50, 200, 250 and 500× magnifications and pore sizes were determined with the ImageJ program.

2.3.4. Swelling measurements

Starch gels were removed from the syringe and cylindrical gel samples were transferred into distilled water at room temperature. The

water was changed daily to remove unreacted components. Swelling kinetics were monitored by weighing the gel samples until they reached equilibrium values.

$$m_{rel} = m_t/m_0 \quad (2)$$

where m_t is the weight of the swollen gel sample at time t and m_0 is the initial weight after preparation [43].

2.3.5. Rheological measumerents

To perform oscillatory measurements, a controlled shear rate rheometer (Physica MCR 102 Anton Paar, Germany) was used with parallel plates. Before initiating the reactions, the gap size (plate diameter 15 mm) was set to 1 mm, and a solvent trap was used during rheological measurements to minimize the evaporation. Gels removed from DMA and VP solution were placed on the glass plate of the rheometer and UV light was transmitted through the photo unit (equipped with Omnicure lamp, 365 nm), thus d-NC gels were synthesized in the rheometer by monitoring the gelation kinetics *in situ*. The fundamental rheological characterization of the networks was conducted using time, frequency, and strain measurements at room temperature. Strain sweeps were performed at a fixed frequency of 1 Hz in the 0.1–100 % strain range to determine the linear viscoelastic region of the samples. Frequency sweeps were conducted at a strain of 0.1 % within the linear viscoelastic region of 0.1–100 Hz. Three replications were made for each measurement to ensure the repeatability of the system.

2.3.6. Compression and elongation measurements

Uniaxial compression and extension tests of s-NC and d-NC-VP gels were performed using a TA.XTplus Texture Analyzer (Stable Micro Systems, Surrey, UK) was equipped with a 5 N load cell, while the d-NC-DMA gel was tested with a 50 N load cell. Compression tests were conducted using cylindrical probes with a height of 5 mm at a rate of 1 mm/min. To ensure the reproducibility of the measurements, at least 7 samples from each gel were tested, and the average values were calculated. Variables and parameters were determined using macros written in the same software. The Young's modulus obtained from the compression tests was calculated from the slope of the stress-strain curves within the deformation range of 5 % to 15 %, corresponding to the linear region.

2.3.7. Loading and in vitro release of protein

After the starch gels reached swelling equilibrium, they were lyophilized, and the dried gels were transferred to 0.05 g/10 mL BSA solutions. For repeatability, 3 samples were used from each gel. The gels were mixed in an oven at 37 °C, 150 rpm for 2 days for protein loading. After loading, the gels were transferred to fresh PBS solutions and placed in a release medium at 37 °C and 150 rpm. At specific time intervals, 500 μL aliquots were collected and replaced with an equal volume of fresh PBS. The collected samples were measured at 562 nm using a microplate reader (BioTek Synergy H1, USA). The unknown BSA concentrations were determined using a calibration curve prepared with known BSA concentrations. The calibration equation with $y = 0.0329\times$ ($R^2 = 0.9991$) was used to determine the BSA concentration. In the next step, to examine the protein release kinetics of the gels in the presence of enzyme, the same procedure was applied using a release medium containing 0.01 g/10 mL α-amylase.

3. Results and discussion

Chemical crosslinkers such as Glutaraldehyde and Epichlorohydrin are frequently used in the preparation of starch-based hydrogels. However, being toxic causes limitations in application areas [44]. Therefore, in this study, single network gels encoded as s-NC were synthesized by cross-linking starch chains with biocompatible and non-toxic, epoxy-functionalized eight-armed g-POSS molecules in order to improve the performance of starch-based hydrogels [45]. In the second step, as illustrated in Fig. 1, to enhance the mechanical properties of the single network, VP and DMA units were polymerized and then crosslinked with BAAm resulting in double network d-NC-VP and d-NC-DMA gels, respectively.

3.1. Gel fraction

The gel fractions, which is calculated to analyze the degree of crosslinking in the network structure of starch gels, is presented in Table 1. The higher amount gel fraction of d-NC-DMA networks compared to s-NC and d-NC-VP gels, as reported in the studies, shows that d-NC-DMA gels have strong hydrophobic interactions, almost all reaction components are incorporated into the structure and the insolubility of the gel network in water during its expansion [46]. Besides, this limited inclusion of VP into the structure may be explained by the steric hindrance caused by bulky groups [47].

3.2. Ft-IR

The chemical structure of starch gels was characterized using FT-IR spectroscopy. As shown in Fig. 2, the peaks around 3291 cm^{-1} and 2924 cm^{-1} correspond to the stretching vibrations of OH and C—H groups in the starch structure, respectively [48]. The fact that the -OH peak (3291 cm^{-1}) in the spectrum of Hylon VII is smaller compared to the gel network structures is an indication that the OH units on the starch chains react with g-POSS. The peak observed at 1081 cm^{-1} originates from the asymmetric stretching vibrations of the Si-O-Si bridge in the POSS structure [49]. The band around 1648 cm^{-1} represents the absorption peak of the carbonyl group present in DMA, and the peak at 1443 cm^{-1} indicates the bending vibrations of the -C-H group in VP [50,51]. In addition, the fact that the peak belonging to epoxy groups at 910 cm^{-1} in the spectrum of g-POSS is not observed in the spectra of s-NC and d-NC networks indicates that the epoxy units in the g-POSS structure are involved in a reaction [52]. Consequently, the presence of g-POSS in starch chains and the inclusion of VP and DMA in s-NC networks have been demonstrated by means of FT-IR analysis.

3.3. Energy dispersive X-ray spectroscopy (EDX)

To demonstrate the presence and homogeneous distribution of g-POSS units along the network, SEM and EDX analysis corresponding to the elements C, O, and Si were examined. As shown in Fig. 3, the presence of a Si peak in the spectrum, along with a Si map similar to that in the micrograph, indicates the inclusion of g-POSS units into the starch network. Furthermore, the homogeneous distribution of Si on the map reveals an almost equal distribution of the crosslinker throughout the d-NC-DMA network structure.

3.4. Swelling measurements

The swelling kinetics of gels depends on various parameters such as crosslink density and the presence of hydrophilic/hydrophobic groups. It was aimed to polymerize s-NC networks to form a double network after reaching swelling equilibrium in reaction solutions containing VP or DMA units. In this regard, when the time-dependent swelling/shrinkage kinetics of s-NC gels in VP/DMA reaction solutions were investigated, it was observed that, as expected, the s-NC network kept in the reaction solutions shrank and reached weight balance after 6 days of immersion (Fig. 4A). Swelling kinetics of the obtained single- and double-network gels were also monitored in distilled water. When the relative swelling rate (m_{rel}) plot given in Fig. 4B was examined, it was observed that all gels reached swelling equilibrium at the end of the second day, regardless of whether the gels were single or double network. The relative swelling ratio increased from 1.2 % to 1.3 % with

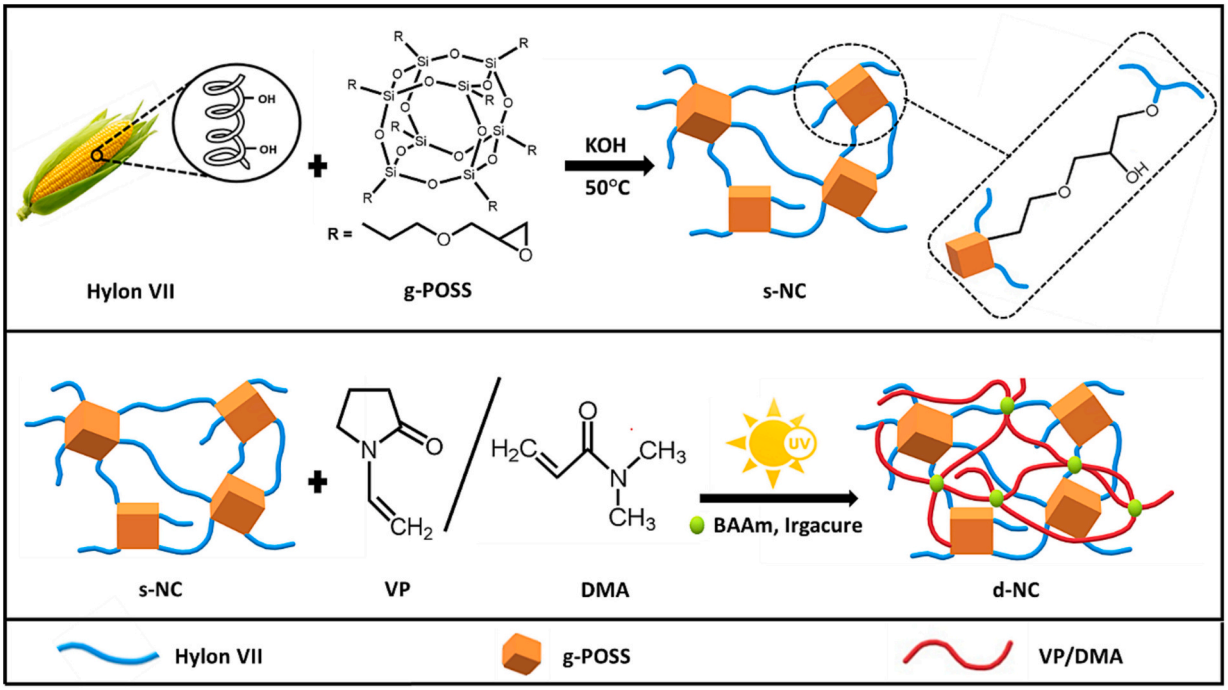

Fig. 1. Schematic illustration of starch gels preparation **A.** Single- nanocomposite (s-NC) prepared with Hylon VII and g-POSS **B.** Double- nanocomposite (d-NC) starch gels prepared with VP/DMA, BAAm and Irgacure in the presence of s-NC.

Table 1
Gel fractions of s-NC and d-NC hydrogels.

Sample code	% Gel fraction
s-NC	72.44 ± 1.77
d-NC-VP	46.59 ± 2.36
d-NC-DMA	96.33 ± 1.29

the addition of VP to the s-NC network and further increased to 2.1 % with the addition of DMA. Incorporation of a second network to the s-NC gel facilitated the adsorption of water molecules by forming additional hydrogen bonds and resulted in a higher adsorption capacity. However, the inability of VP to fully incorporate into the structure led to a significantly lower water retention capacity compared to the d-NC-DMA gel.

3.5. Rheological measurements

For *in situ* monitoring the gelation reactions, the reaction solution of s-NC gel was transferred between the plates of the rheometer. However, due to the slow rate of reactions that caused the samples to dry on the rheometer, *in situ* monitoring could not be applied to the s-NC networks. Therefore, the s-NC gel was obtained in an oven at 50 °C instead of a rheometer. To monitor the formation of the second network *in situ,* s-NC gels soaked in VP/DMA solutions containing crosslinker and photo-initiator for 3 days were placed between the plates of the rheometer. The storage modulus (G') and loss modulus (G'') of the system were followed for 5 min using oscillating deformation measurements under $f = 1$ Hz constant frequency and $\gamma = 0.1$ stress amplitude, followed by exposure to 365 nm UV light throughout the reaction. As shown in Fig. 5, there was a sudden increase in the modulus of DMA and VP gels, and after 15 min of irradiation, the G' and G'' values were recorded as 54.5 kPa and 5.4 kPa for d-NC-DMA, and 9.6 kPa and 1.1 kPa for d-NC-VP gels, respectively. Additionally, it was observed that the DMA system exhibited faster reaction kinetics. The d-NC-DMA gel has been shown to have a superior modulus value compared to the reported mechanically enhanced starch gels [53–55]. G' and G'' values of the s-NC gel synthesized in the oven and containing no photoinitiator were determined to be approximately 1.5 kPa and 0.1 kPa, respectively. As expected, did not change in modulus values was observed when exposure to UV light as applied to the d-NC gels.

Fig. 6 shows the deformation plot of the G' and G'' values at 0.1 % to 100 % strain at a fixed frequency of 1 Hz. While the modulus of the d-NC-VP gel increased compared to the s-NC, sol-gel transitions were observed when shear deformation of about 7 % was applied. On the other hand, in s-NC, the sol-gel transition occurred at approximately 25 % shear deformation. This means that the d-NC-VP gel breaks down at much lower deformation values compared to the s-NC structure. It has been observed that with the incorporation of DMA into the s-NC networks, the LVR range is significantly expanded, and it is stable up to 100 % strain. This can be interpreted as evidence of higher stability and better mechanical properties compared to s-NC and d-NC-VP gel.

3.6. Scanning electron microscopy

SEM images of s-NC, d-NC-DMA, and d-NC-VP gels were taken after swelling and lyophilization processes as shown in Fig. 7. According to the images, the first point to notice is that all starch gels exhibit a porous structure. It was observed that the pore sizes decreased in the d-NC-VP and d-NC-DMA gels obtained by incorporating DMA and VP into the s-NC network [56,57]. While the pore size in s-NC is 175 ± 45 μm, it decreases to 135 ± 65 μm and 120 ± 37 μm in d-VP and d-DMA, respectively. The difference in pore size of the double network gels can be attributed to the inability of VP to fully penetrate the structure due to steric hindrance, as also observed in the gel fraction. Another important point is that the presence of the second network in the d-NC-DMA structure has a stronger effect on the pore wall thickness. As expected, this effect results in increased mechanical strength in d-NC-DMA nanocomposite hydrogels.

3.7. Compression and elongation measurements

One of the important issues in drug delivery systems is that the drug has improved mechanical strength in such a way that it can be easily

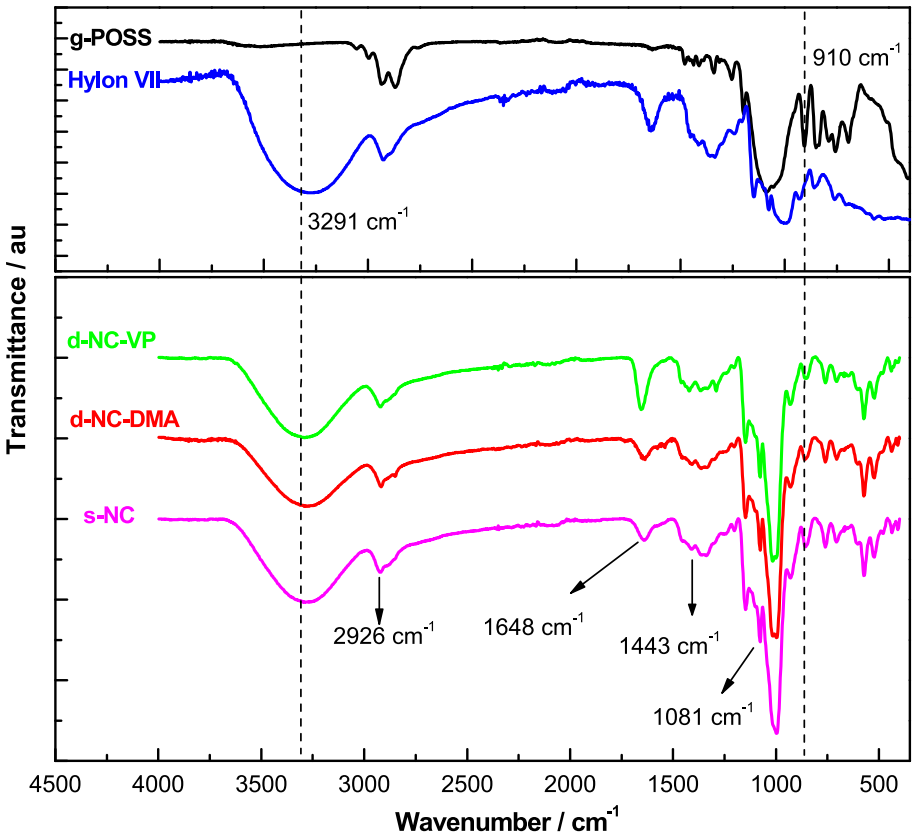

Fig. 2. FT-IR spectrum of g-POSS, Hylon VII, s-NC and d-NC starch gels after lyophilization.

transported in the carrier while preserving its structure [58,59]. Chavda et al. investigated the mechanical strength of the superporous hydrogels in drug delivery systems in order to withstand the expected pressure in the stomach during repeated gastric contractions [60]. In order to use the starch gels obtained in this direction as a durable carrier system, their mechanical strength was determined using uniaxial elongation and compression tests using a Texture Analyzer. s-NC starch gel could not even be placed in the device to perform elongation measurement due to its brittle structure. d-NC-VP starch gels broke as soon as the test started after being placed between the jaws of the device (Fig. 8A). In contrast, elongation measurements of the d-NC-DMA starch gel were quantitatively determined, and the increase in deformation resulted in increased elongation strength and toughness (Fig. 8B). As a result of the measurement, it was determined that it had an elongation at a break of 116 ± 8 % and a strength of 60 ± 14 kPa.

When uniaxial compression tests are examined, Fig. 9A shows the stress-strain curves of cylindrical gel samples at 24 °C. Similar to the rheological analysis results, the initial slope of the curves, Young's Modulus *E*, was 7 ± 1 kPa in s-NC and 31 ± 8 kPa in d-NC-VP gel, while d-NC-DMA gel had the highest modulus with 760 ± 125 kPa (Fig. 9B). However, the maximum force value, σ_f to disrupt the structural integrity of the gels decreased from 5 kPa to 1.6 kPa in x d-NC-VP gel compared to the s-NC network. With the inclusion of DMA, the mechanical strength of the gel increased and the maximum deformation value that the gel could withstand, λ_f, increased, as well as σ_f increased from kPa to MPa and was recorded as 5.4 + 0.2 MPa. While determining the σ_f and λ values in Fig. 9B, the transition from nominal values to true values is made, and the equation $\sigma_{true} = \lambda\, \sigma_{nom}$ is used as a function of the strain rate (λ) [61]. The photographs of the gels before and after compression tests qualitatively clearly show that the d-NC-DMA gels have a much stronger mechanical structure. In the video of the d-NC-DMA gel, when pinched between two fingers, the gel sample preserves its macro structure without breaking down (Supp. video). When the studies with many starch gels obtained by using different crosslinkers reported in the literature are examined, it can be said that the d-NC-DMA gel has a superior Young's Modulus value [40,62–65].

3.8. *In vitro release of protein*

Based on the idea of using the designed starch gels for protein release as a potential application area, experiments were carried out with the model protein BSA. Many studies using BSA as a model protein in protein release studies of hydrogels have been reported [66–68]. BSA is a valuable alternative to human serum albumin (HSA) due to its medical importance, low cost, high availability and approximately 76 % similarity to HSA in its molecular structure [69]. The release process consists of 3 steps: absorbing the protein into the lyophilized gel, monitoring the release kinetics in environments with and without enzyme. Firstly, *in vitro* release medium was created for BSA-loaded gels and samples were taken from the release medium at regular intervals and monitored for more than two weeks. As seen in the Fig. 10A, a negligible level of BSA was released for 16 days, regardless of the network type, and almost all of the protein was retained in the structure. In detail, 1.80 %, 1.40 % and 1.05 % protein were released from s-NC, d-NC-VP and d-NC-DMA gels, respectively. By introducing second networks into the s-NC gel, the pore sizes were reduced, resulting in a decrease in protein release. The results suggest that pore size plays an important role in protein release.

Actual release was performed in a medium containing α-amylase enzyme, which catalyzes the hydrolysis of starch, to complete the release process of BSA from the starch networks (Fig. 10B) [35]. Since amylase breaks down starch units, s-NC structures are expected to have the fastest protein release kinetics among the 3 different gel systems. In Fig. 10B, it was determined that the release of BSA from the s-NC gels occurred in 4 h, while the release from the d-NC-VP gels was completed in 1.5 h. Additionally, it is also shown by the photographs in Fig. S1 that the initially transparent medium begins to turbid with degradation and

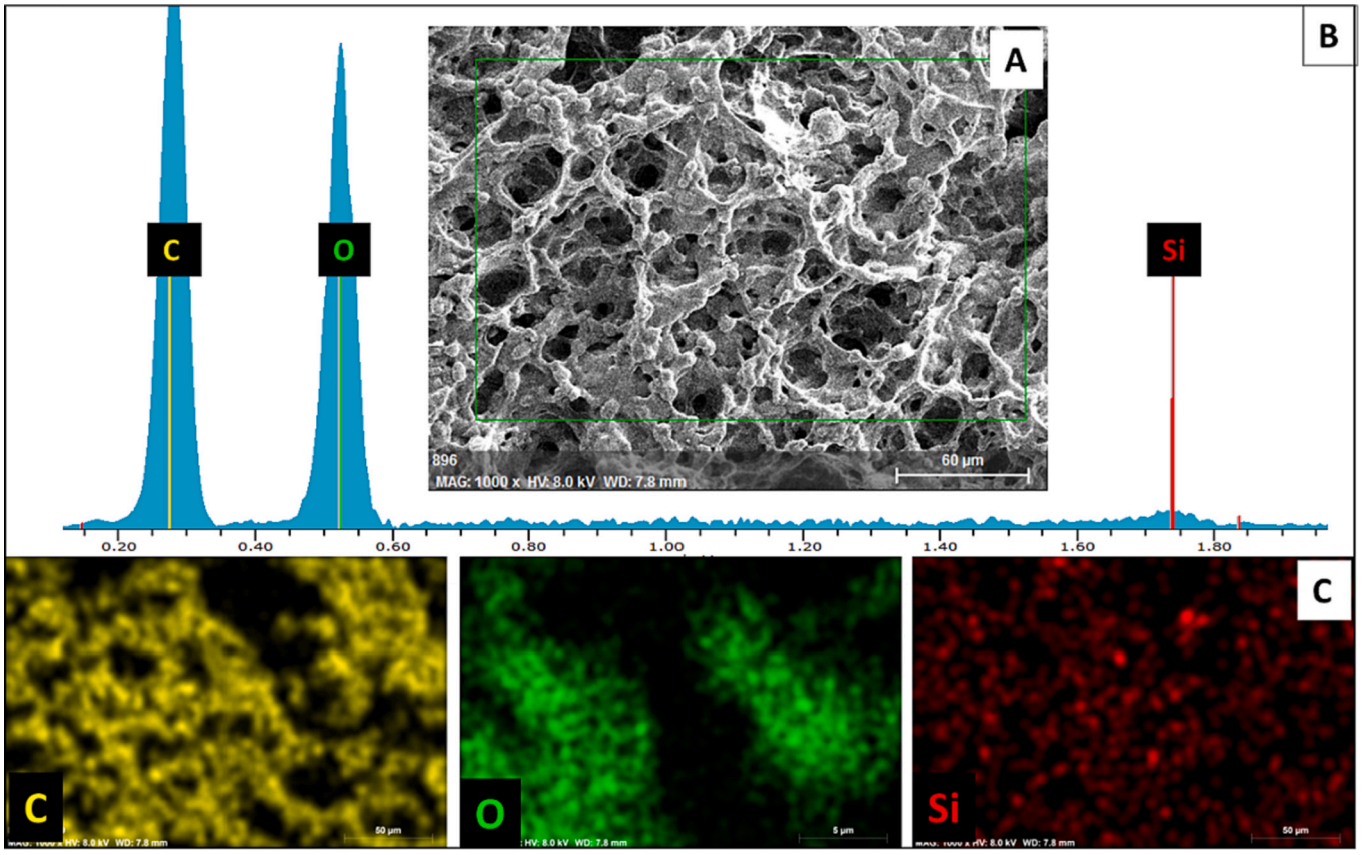

Fig. 3. **A.** Scanning electron microscopy (SEM) micrograph and **B.** their corresponding energy dispersive X-ray spectroscopy (EDX) analytical spectra and **C.** map of C, O and Si for the d-NC-DMA gel.

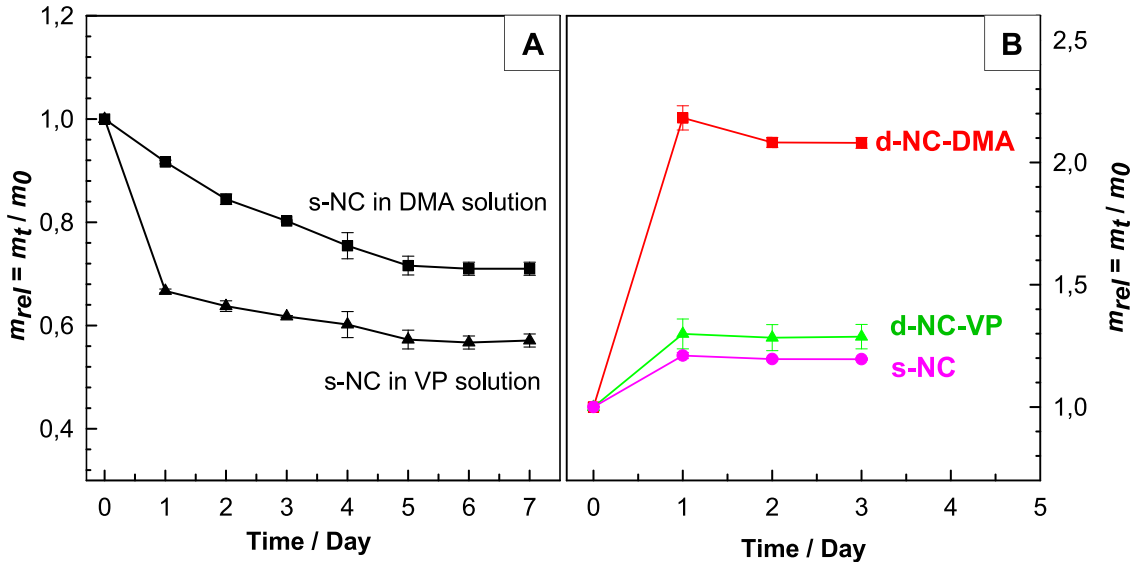

Fig. 4. Relative swelling *versus* time plots **A.** s-NC gels in reaction solutions containing VP or DMA units **B.** s-NC and d-NC gels in distilled water.

the turbidity increases with time correlated with the release kinetics. This suggests that insoluble protein particles are formed in the environment along with the structural changes in the gel, and these particles disperse in the environment during the release process.

Before starting the release process, the pH values of the solutions were measured and determined to be 6.7. After 1 h of release, the pH values were examined, and the pH of s-NC was measured as 7.2, while the pH of d-NC-VP was measured as 6.9. The pH value of 6.9 for the d-NC-VP gel within the optimum pH range (6.7–7.0) where α-amylase functions properly as an enzyme [70]. This explains why the d-NC-VP starch gel degrades and releases proteins faster compared to the s-NC gel. Although the pH of the d-NC-DMA gel measured after 1 h is close to the optimum range (pH = 7.08), it shows greater resistance to α-amylase due to the higher mechanical strength of the network structure than

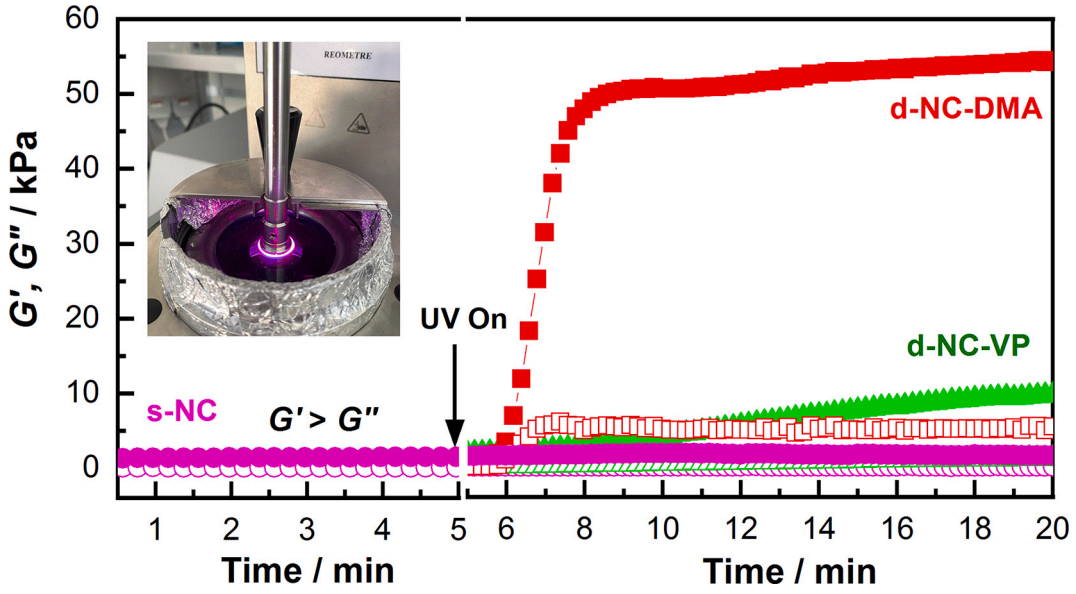

Fig. 5. Storage modulus (*G'*, filled symbol) and loss modulus (*G"*, open symbol) of the s-NC gels prepared outside the rheometer. *G'* and *G" versus* time plot of s-NC and s-NC immersed into the VP and DMA reaction solution under 365 nm UV irradiation (●; s-NC, ▲; d-NC-VP, ■; d-NC-DMA).

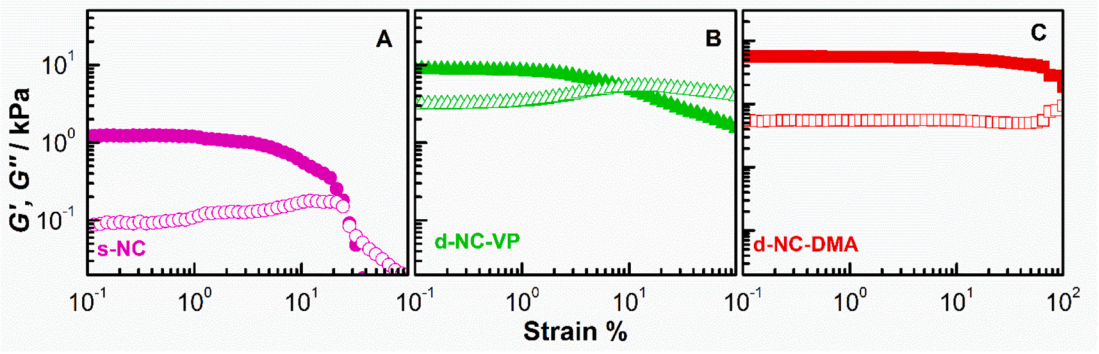

Fig. 6. Shear deformation tests of starch gels. **A.** ●; s-NC, **B.** ▲; d-NC-VP, **C.** ■; d-NC-DMA. *G'* and *G"* are represented by filled and open symbols, respectively.

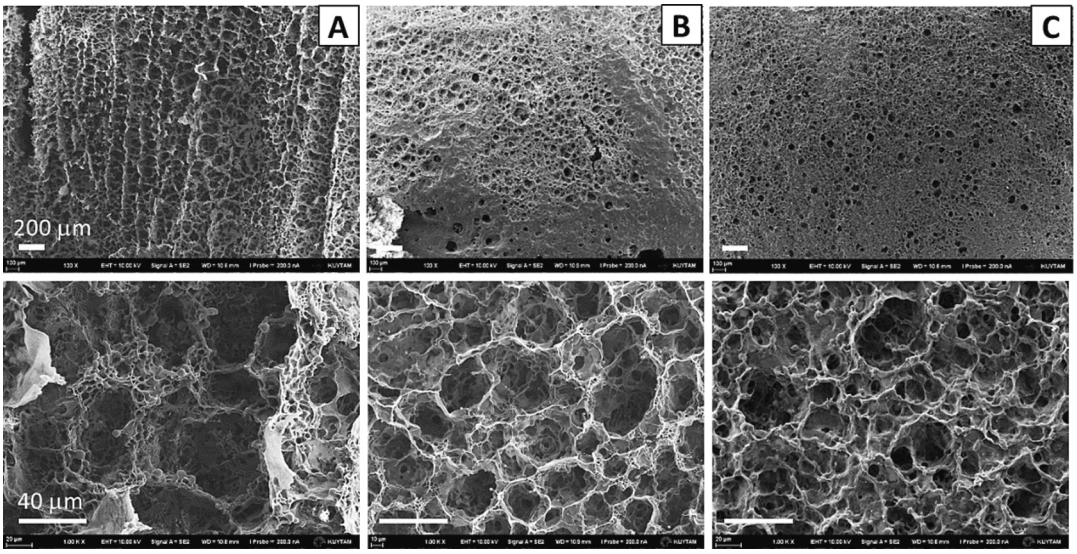

Fig. 7. SEM images of **A.** s-NC, **B.** d-NC-VP and **C.** d-NC-DMA starch gels. 100× (upper level, with 200 µm scale bar) and 1000× magnifications (lower level, with 40 µm scale bar).

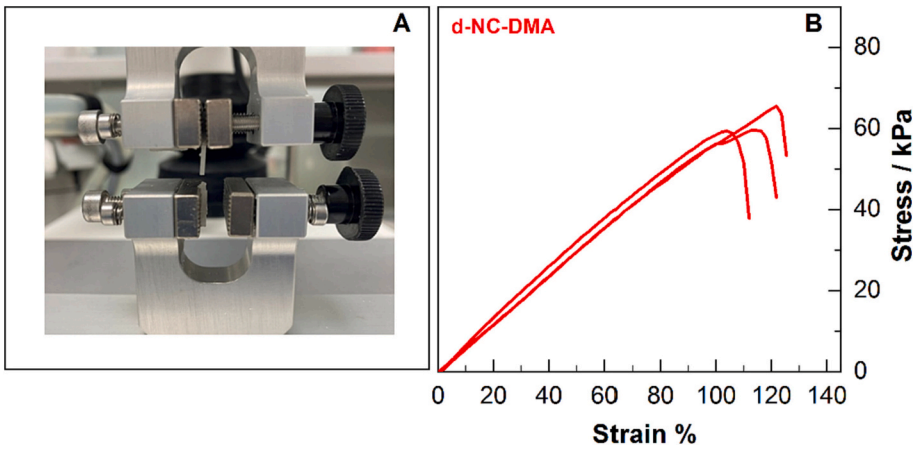

Fig. 8. **A.** Rupture of the d-NC-VP starch gel during tensile test. **B.** Stress-strain curves of d-NC-DMA starch gels.

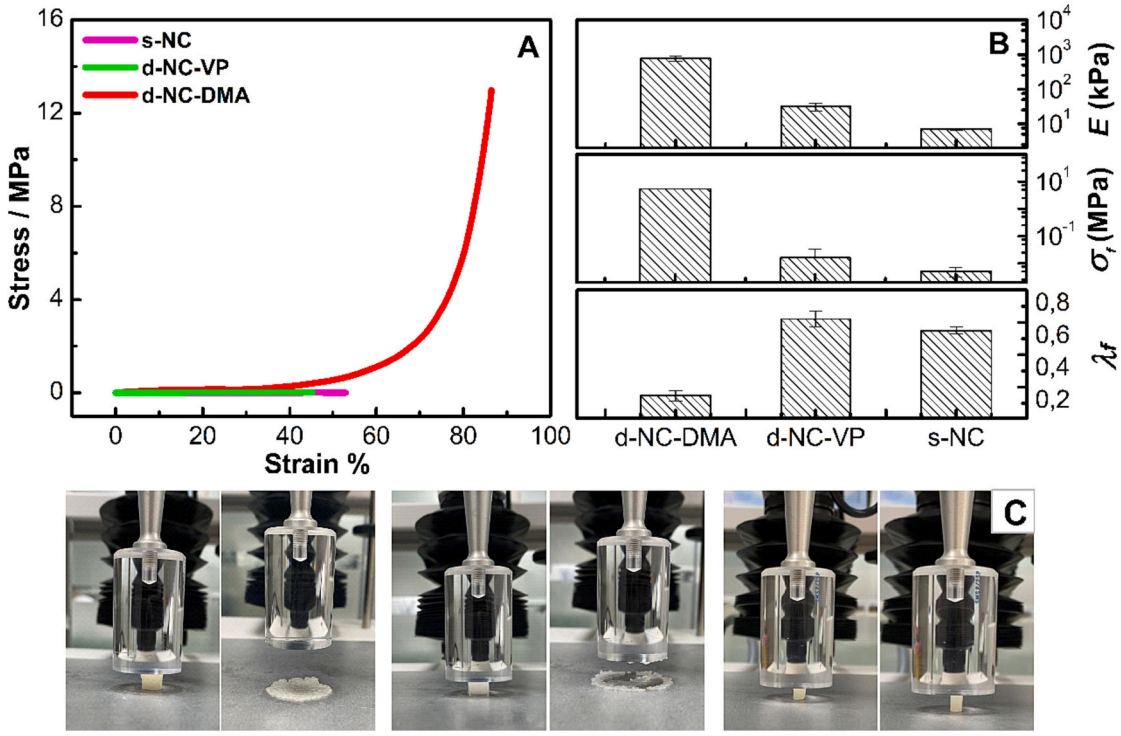

Fig. 9. Compression tests of starch gels **A.** typical stress-strain curve of the measurement, **B.** Averages of Young's modulus *E*, breaking stress σ_f, breaking deformation λ_f, **C.** Photographs of gels before and after compression tests.

other starch gels. While this gel achieves 29 % release in 6 h, the release percentage remains constant thereafter, indicating that the entire protein within the gel network has not been released.

4. Conclusions

Starting from starch, which is one of the most used natural polymers in hydrogel synthesis, which has advantages such as easy availability and low cost, single network (s-NC) and double network (d-NC) nanocomposite starch gels were synthesized in the presence of 8-armed cubic g-POSS as a crosslinker. The structures s-NC, d-NC-VP and d-NC-DMA obtained by combining the strategies to obtain double network and nanocomposite gels to enhance mechanical strength were compared.

First, it was proved by FT-IR and EDX analyzes that g-POSS is included in the gel structure and is homogeneously distributed throughout the network structure. The characterization studies of the gels showed that d-NC-DMA possesses superior properties compared to s-NC and d-NC-VP starch gels. The formation of the secondary network was followed *in situ* on the rheometer using oscillatory deformation measurements at a constant frequency $f = 1$ Hz and amplitude $\gamma = 0.1$. The storage modulus of s-NC gels, *G'*, which was 1.5 kPa, increased with UV irradiation in DMA and VP reaction solutions and was recorded as 54.46 and 9.6 kPa, respectively, for d-NC-DMA and d-NC-VP gels. The d-NC-DMA gel has been shown to have a superior modulus value compared to the reported mechanically enhanced starch gels on the literature. Additionally, it was observed that the DMA system exhibited faster reaction kinetics. SEM analyzes demonstrated that the pore sizes of s-NC gels were reduced by incorporating DMA and VP units as a second network. When the pore walls of the double network gels were compared, it was determined that the d-NC-DMA structure had thicker walls resulting in much better mechanical strength of the respective gels compared to the d-NC-VP networks. In addition, the larger linear

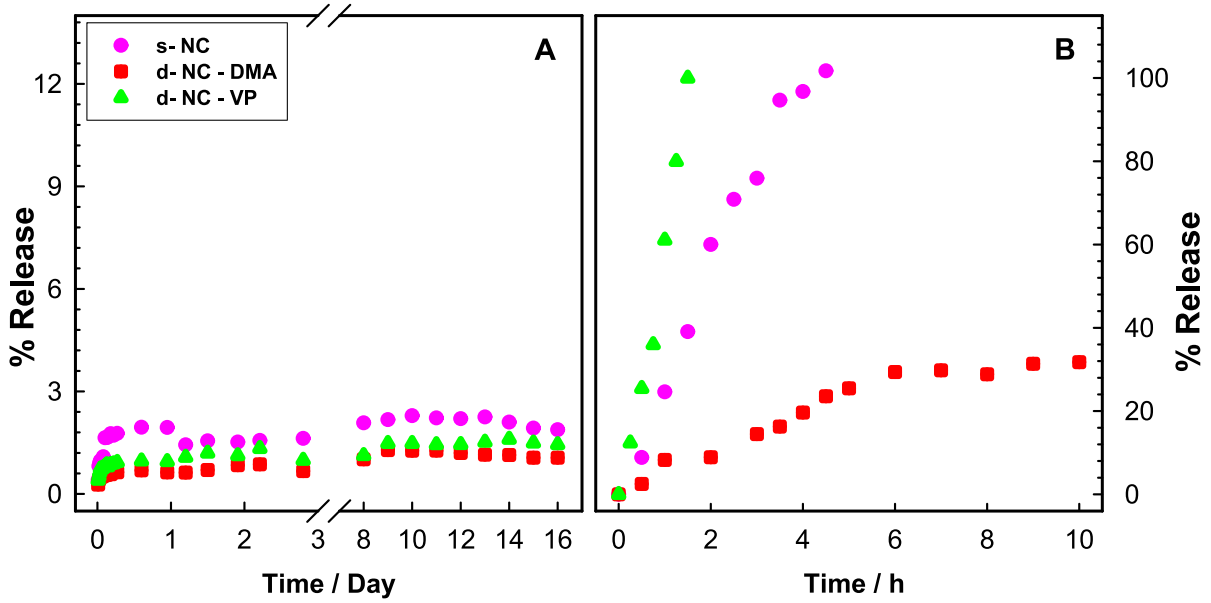

Fig. 10. Time-dependent bovine serum albumin (BSA) release from starch gels **A.** in the absence and **B.** presence of α-amylase molecules.

viscoelastic region (LVER) observed in the deformation sweep and the Young's modulus value of approximately 100-fold and 25-fold higher, respectively, compared to the s-NC and d-NC-VP networks obtained from the uniaxial compression test also indicated the durability of the d-NC-DMA gels.

In the last part, *in vitro* experiments were carried out to use the designed gels for protein release as an application. While the gels loaded with the model protein BSA trap their load in the network, they break down in the presence of α-amylase, which catalyzes starch, and protein is released within hours. In conclusion, this study is promising for future studies of protein or drug release in α-amylase-rich environments. In addition, the high mechanical strength of the gels to be used in these systems is very important in terms of delivering the drug/protein to the target area in the body without disturbing its structure.

Supplementary data to this article can be found online at https://doi.org/10.1016/j.ijbiomac.2023.128705.

CRediT authorship contribution statement

Seyma Nur Kirmic Cosgun: Conceptualization, Data curation, Methodology, Visualization, Writing – original draft, Writing – review & editing. **Deniz Ceylan Tuncaboylu:** Conceptualization, Data curation, Funding acquisition, Project administration, Supervision, Validation, Visualization, Writing – original draft, Writing – review & editing. **Mahinur Alemdar:** Methodology.

Declaration of competing interest

The authors declare the following financial interests/personal relationships which may be considered as potential competing interests: D. C.T. reports financial support was provided by Drug Application and Research Center (ILMER) at Bezmialem Vakif University. D.C.T. reports financial support was provided by Turkish Academy of Sciences (TUBA). S.N.K.C. thanks the Scientific and Technological Research Council of Turkey (TÜBİTAK) for the scholarship support.

Acknowledgments

This work is a part of Seyma Nur Kirmiç Cosgun's MSc dissertation. The authors acknowledge resources and support from the Drug Application and Research Center (ILMER) at Bezmialem Vakif University. D. C.T. thanks the Turkish Academy of Sciences (TUBA) for the support. S. N.K.C. thanks the Scientific and Technological Research Council of Turkey (TÜBİTAK) for the scholarship support.

References

[1] C.-J. Wu, et al., Mechanically tough pluronic F127/laponite nanocomposite hydrogels from covalently and physically cross-linked networks, Macromolecules 44 (20) (2011) 8215–8224.
[2] P. Prakash, M. Porwal, A. Saxena, Role of natural polymers in sustained release drug delivery system: application and recent approaches, Int. Res. J. Pharm. 2 (9) (2011) 6–11.
[3] A.S. Hoffman, Hydrogels for biomedical applications, Adv. Drug Deliv. Rev. 64 (2012) 18–23.
[4] C. Chang, L. Zhang, Cellulose-based hydrogels: present status and application prospects, Carbohydr. Polym. 84 (1) (2011) 40–53.
[5] H. Mittal, S.S. Ray, M. Okamoto, Recent progress on the design and applications of polysaccharide-based graft copolymer hydrogels as adsorbents for wastewater purification, Macromol. Mater. Eng. 301 (5) (2016) 496–522.
[6] T. Funami, et al., Food hydrocolloids control the gelatinization and retrogradation behavior of starch. 2a. Functions of guar gums with different molecular weights on the gelatinization behavior of corn starch, Food Hydrocoll. 19 (1) (2005) 15–24.
[7] H. Zobel, Molecules to granules: a comprehensive starch review, Starch-Stärke 40 (2) (1988) 44–50.
[8] J.J. Van Soest, et al., Crystallinity in starch bioplastics, Ind. Crop. Prod. 5 (1) (1996) 11–22.
[9] M.M. Zohourian, K. Kabiri, Superabsorbent Polymer Materials: A Review, 2008.
[10] S.C. Alcázar-Alay, M.A.A. Meireles, Physicochemical properties, modifications and applications of starches from different botanical sources, Food Sci. Technol. 35 (2015) 215–236.
[11] D. Ceylan Tuncaboylu, S. Abdurrahmanoglu, I. Gazioglu, Rheological characterization of starch gels: a biomass based sorbent for removal of polycyclic aromatic hydrocarbons (PAHs), J. Hazard. Mater. 371 (2019) 406–414.
[12] L. Kuniak, R. Marchessault, Study of the crosslinking reaction between epichlorohydrin and starch, Starch-Stärke 24 (4) (1972) 110–116.
[13] K. Manoi, S.S. Rizvi, Physicochemical characteristics of phosphorylated cross-linked starch produced by reactive supercritical fluid extrusion, Carbohydr. Polym. 81 (3) (2010) 687–694.
[14] L. Ren, et al., Dual modification of starch nanocrystals via crosslinking and esterification for enhancing their hydrophobicity, Food Res. Int. 87 (2016) 180–188.
[15] S. Roberts, R. Cameron, The effects of concentration and sodium hydroxide on the rheological properties of potato starch gelatinisation, Carbohydr. Polym. 50 (2) (2002) 133–143.
[16] H. Luo, et al., Construction of porous starch-based hydrogel via regulating the ratio of amylopectin/amylose for enhanced water-retention, Molecules 26 (13) (2021) 3999.
[17] F.M. Carbinatto, et al., Physical properties of pectin–high amylose starch mixtures cross-linked with sodium trimetaphosphate, Int. J. Pharm. 423 (2) (2012) 281–288.
[18] G. Liu, et al., Effects of molecular interactions in debranched high amylose starch on digestibility and hydrogel properties, Food Hydrocoll. 101 (2020), 105498.

[19] G. Feltre, et al., Alginate and corn starch mixed gels: effect of gelatinization and amylose content on the properties and in vitro digestibility, Food Res. Int. 132 (2020), 109069.
[20] J.P. Gong, et al., Double-network hydrogels with extremely high mechanical strength, Adv. Mater. 15 (14) (2003) 1155–1158.
[21] Y. Tanaka, J.P. Gong, Y. Osada, Novel hydrogels with excellent mechanical performance, Prog. Polym. Sci. 30 (1) (2005) 1–9.
[22] K. Haraguchi, T. Takehisa, Nanocomposite hydrogels: a unique organic–inorganic network structure with extraordinary mechanical, optical, and swelling/de-swelling properties, Adv. Mater. 14 (16) (2002) 1120–1124.
[23] O. Okay, Polymeric Cryogels: Macroporous Gels With Remarkable Properties 263, Springer, 2014.
[24] S. Liu, et al., POSS hybrid hydrogels: a brief review of synthesis, properties and applications, Eur. Polym. J. 143 (2021), 110180.
[25] Y. Chen, et al., POSS hybrid robust biomass IPN hydrogels with temperature responsiveness, Polymers 11 (3) (2019) 524.
[26] E. Franchini, et al., Influence of POSS structure on the fire retardant properties of epoxy hybrid networks, Polym. Degrad. Stab. 94 (10) (2009) 1728–1736.
[27] R.M. Laine, et al., Polyfunctional cubic silsesquioxanes as building blocks for organic/inorganic hybrids, Appl. Organomet. Chem. 12 (10−11) (1998) 715–723.
[28] J. Shen, et al., Hydrolytically degradable POSS-PEG hybrid hydrogels prepared in aqueous phase with tunable mechanical properties, swelling ratio and degradation rate, React. Funct. Polym. 123 (2018) 91–96.
[29] Y. Zhang, et al., In situ bone regeneration enabled by a biodegradable hybrid double-network hydrogel, Biomater. Sci. 7 (8) (2019) 3266–3276.
[30] G. Hou, et al., Preparation and characterization of nanocomposite films by hybrid cationic ring opening polymerization of glycidyl-POSS, Mater. Chem. Phys. 148 (1) (2014) 236–244.
[31] D.V. Goeddel, et al., Expression in Escherichia coli of chemically synthesized genes for human insulin, Proc. Natl. Acad. Sci. 76 (1) (1979) 106–110.
[32] V. Lee, Enzymatic barriers to peptide and protein absorption, Crit. Rev. Ther. Drug Carrier Syst. 5 (2) (1988) 69–97.
[33] F.A. Dorkoosh, et al., Evaluation of superporous hydrogel (SPH) and SPH composite in porcine intestine ex-vivo: assessment of drug transport, morphology effect, and mechanical fixation to intestinal wall, Eur. J. Pharm. Biopharm. 53 (2) (2002) 161–166.
[34] T. Vermonden, R. Censi, W.E. Hennink, Hydrogels for protein delivery, Chem. Rev. 112 (5) (2012) 2853–2888.
[35] L.K. Fung, W.M. Saltzman, Polymeric implants for cancer chemotherapy, Adv. Drug Deliv. Rev. 26 (2–3) (1997) 209–230.
[36] V.R. Sinha, R. Kumria, Polysaccharides in colon-specific drug delivery, Int. J. Pharm. 224 (1–2) (2001) 19–38.
[37] P. Ravichandran, K. Shantha, K.P. Rao, Preparation, swelling characteristics and evaluation of hydrogels for stomach specific drug delivery, Int. J. Pharm. 154 (1) (1997) 89–94.
[38] J. Heller, Use of enzymes and bioerodible polymers in self-regulated and triggered drug delivery systems, in: Pulsed and Self-regulated Drug Delivery, CRC Press Boca Raton, FL, 1990, pp. 93–108.
[39] J. Kost, S. Shefer, Chemically-modified polysaccharides for enzymatically-controlled oral drug delivery, Biomaterials 11 (9) (1990) 695–698.
[40] M. Alemdar, D. Ceylan Tuncaboylu, Rheological analysis of polysaccharide hydrogels, Starch-Stärke 73 (3–4) (2021), 2000198.
[41] N.-P.-D. Tran, M.-C. Yang, Synthesis and characterization of silicone contact lenses based on TRIS-DMA-NVP-HEMA hydrogels, Polymers 11 (6) (2019) 944.
[42] M. Wu, et al., Irradiation of crosslinked, poly (vinyl alcohol) blended hydrogel for wound dressing, J. Radioanal. Nucl. Chem. 250 (2) (2001) 391–395.
[43] S.N.K. Cosgun, D.C. Tuncaboylu, Cyclodextrin-linked PVP/PEG supramolecular hydrogels, Carbohydr. Polym. 269 (2021), 118278.
[44] C. Cui, et al., Recent advances in the preparation, characterization, and food application of starch-based hydrogels, Carbohydr. Polym. 291 (2022), 119624.
[45] J. Ozimek, K. Pielichowski, Recent advances in polyurethane/POSS hybrids for biomedical applications, Molecules 27 (1) (2021) 40.
[46] M.P. Algi, O. Okay, Highly stretchable self-healing poly (N, N-dimethylacrylamide) hydrogels, Eur. Polym. J. 59 (2014) 113–121.
[47] Doda, A., et al., Investigation of alkali and salt resistant copolymer of acrylic acid and N-vinyl-2-pyrrolidinone for medium viscosity oil recovery. Can. J. Chem. Eng.
[48] A. Odiongenyi, N. Essien, R. Ukpe, Corn starch as a substitute for commercial food starch: FT-IR and rheological characterization, J. Sci. Eng. Res. 3 (6) (2016) 494–501.
[49] B. Wang, et al., Polyhedral oligomeric silsesquioxane (POSS)-modified phenolic resin: synthesis and anti-oxidation properties, e-Polymers 21 (1) (2021) 316–326.
[50] Y. Liu, et al., Thio-Michael addition of α, β-unsaturated amides catalyzed by Nmm-based ionic liquids, RSC Adv. 7 (68) (2017) 43104–43113.
[51] P. Vasudevan, et al., Synthesis and structural characterization of sol–gel derived titania/poly (vinyl pyrrolidone) nanocomposites, J. Sol-Gel Sci. Technol. 62 (2012) 41–46.
[52] W. Li, et al., Fabrication and investigations of G-POSS/cyanate ester resin composites reinforced by silane-treated silica fibers, Compos. Sci. Technol. 173 (2019) 7–14.
[53] Q. Lin, et al., Self-healing, stretchable, and freezing-resistant hydroxypropyl starch-based double-network hydrogels, Carbohydr. Polym. 251 (2021), 116982.
[54] X. Chen, et al., Dual Cross-Linked Starch–Borax Double Network Hydrogels with Tough and Self-Healing Properties, Foods 11 (9) (2022) 1315.
[55] J. Lu, et al., Highly tough, freezing-tolerant, healable and thermoplastic starch/poly (vinyl alcohol) organohydrogels for flexible electronic devices, J. Mater. Chem. A 9 (34) (2021) 18406–18420.
[56] M.A. Haque, T. Kurokawa, J.P. Gong, Super tough double network hydrogels and their application as biomaterials, Polymer 53 (9) (2012) 1805–1822.
[57] Y. Li, et al., Fabrication of CS/SA double-network hydrogel and application in pH-controllable drug release, ChemistrySelect 4 (48) (2019) 14036–14042.
[58] P. Gupta, K. Vermani, S. Garg, Hydrogels: from controlled release to pH-responsive drug delivery, Drug Discov. Today 7 (10) (2002) 569–579.
[59] S. Sharma, P. Jain, S. Tiwari, Dynamic imine bond based chitosan smart hydrogel with magnified mechanical strength for controlled drug delivery, Int. J. Biol. Macromol. 160 (2020) 489–495.
[60] H. Chavda, C. Patel, Effect of crosslinker concentration on characteristics of superporous hydrogel, Int. J. Pharm. Investig. 1 (1) (2011) 17.
[61] H. Kılıç, et al., Design of biocompatible multifunctional hydrogels with stearyl methacrylate and vinylpyrrolidone, ACS Appl. Polym. Mater. 4 (3) (2022) 1717–1727.
[62] J. Sringam, et al., Improving mechanical properties of starch-based hydrogels using double network strategy, Polymers 14 (17) (2022) 3552.
[63] S. Konstantakos, et al., Preparation of model starch complex hydrogels, Food Hydrocoll. 96 (2019) 365–372.
[64] S. Zeng, et al., Transparent, flexible, and multifunctional starch-based double-network hydrogels as high-performance wearable electronics, Carbohydr. Polym. 267 (2021), 118198.
[65] J. Arayaphan, et al., Synthesis of photodegradable cassava starch-based double network hydrogel with high mechanical stability for effective removal of methylene blue, Int. J. Biol. Macromol. 168 (2021) 875–886.
[66] A. Salama, Chitosan based hydrogel assisted spongelike calcium phosphate mineralization for in-vitro BSA release, Int. J. Biol. Macromol. 108 (2018) 471–476.
[67] A. Naddaf, I. Tsibranska, H.-J. Bart, Kinetics of BSA release from poly (N-isopropylacrylamide) hydrogels, Chem. Eng. Process. Process Intensif. 49 (6) (2010) 581–588.
[68] S. Sarıyer, et al., pH-responsive double network alginate/kappa-carrageenan hydrogel beads for controlled protein release: effect of pH and crosslinking agent, J. Drug Deliv. Sci. Technol. 56 (2020), 101551.
[69] S.T.K. Raja, et al., pH and redox sensitive albumin hydrogel: a self-derived biomaterial, Sci. Rep. 5 (1) (2015), 15977.
[70] P. Vijayaraghavan, C. Remya, S.P. Vincent, Production of [alpha]-amylase by Rhizopus microsporus using agricultural by-products in solid state fermentation, Res. J. Microbiol. 6 (4) (2011) 366.